Encapsulation of mRNA into Artificial Viral Capsids via Hybridization of a *β*-Annulus-dT$_{20}$ Conjugate and the Poly(A) Tail of mRNA

Yoko Nakamura [1], Yuki Sato [1], Hiroshi Inaba [1,2], Takashi Iwasaki [3] and Kazunori Matsuura [1,2,*]

[1] Department of Chemistry and Biotechnology, Graduate School of Engineering, Tottori University, Tottori 680-8552, Japan; yotasa0926@gmail.com (Y.N.); yuki.s09hr@gmail.com (Y.S.); hinaba@tottori-u.ac.jp (H.I.)

[2] Centre for Research on Green Sustainable Chemistry, Tottori University, Tottori 680-8552, Japan

[3] Department of Bioresources Science, Graduate School of Agricultural Sciences, Tottori University, Tottori 680-8553, Japan; itaka@tottori-u.ac.jp

* Correspondence: ma2ra-k@tottori-u.ac.jp; Tel.: +81-857-31-5262

Abstract: Messenger RNA (mRNA) drugs have attracted considerable attention as promising tools with many therapeutic applications. The efficient delivery of mRNA drugs using non-viral materials is currently being explored. We demonstrate a novel concept where mCherry mRNA bearing a poly(A) tail is encapsulated into capsids co-assembled from viral *β*-annulus peptides bearing a 20-mer oligothymine (dT$_{20}$) at the N-terminus and unmodified peptides via hybridization of dT$_{20}$ and poly(A). Dynamic light scattering measurements and transmission electron microscopy images of the mRNA-encapsulated capsids show the formation of spherical assemblies of approximately 50 nm. The encapsulated mRNA shows remarkable ribonuclease resistance. Further, modification by a cell-penetrating peptide (His16) on the capsid enables the intracellular expression of mCherry of encapsulated mRNA.

Keywords: mRNA; poly(A) tail; artificial viral capsid; encapsulation; nanocapsule; self-assembly; *β*-annulus peptide; peptide-DNA conjugate

1. Introduction

Therapeutic mRNA have attracted attention in recent years as a new type of nucleic acid drugs. Such mRNAs show potential for use in protein replacement therapy and vaccination [1–6]. mRNA drugs have the advantage of inducing direct protein synthesis in the cytoplasm, thus differing from DNA therapy. Naked mRNA is; however, unstable outside of cells and is unable to effectively penetrate cell membranes due to electrostatic repulsion. Thus, various materials for mRNA delivery, such as liposomes, dendrimers, and polyion complex micelles, have been developed and are attractive for their flexibility in molecular design [2–11]. Conversely, RNA viruses package specific genome molecules inside their outer protein shell, the viral capsid [12,13]. Viral capsids are also attractive for precise mRNA packaging and delivery but the use of natural viruses for mRNA delivery has safety concerns. Virus-like artificial protein cages for RNA packaging are, therefore, attractive. Recently, Hilvert and coworkers demonstrated that a non-viral protein cage formed by *Aquifex aeolicus* lumazine synthase selectively packages mRNA via cationic peptide tags [14,15].

Eukaryotic mRNA possesses a long adenine nucleotide (poly(A)) tail of about 100~200 nt at the 3′-end to regulate translation [16–21]. We propose a novel strategy for the encapsulation of mRNA into virus-like peptide nanocapsules via hybridization between dT$_{20}$ and the poly(A) tails. We developed an "artificial viral capsid" with a size of 30–50 nm self-assembled from the *β*-annulus

peptide (INHVGGTGGAIMAPVAVTRQLVGS) that participates in the formation of the dodecahedral internal skeleton of the tomato bushy stunt virus [22–35]. Artificial viral capsids encapsulate anionic guest molecules and His-tagged green fluorescence protein (GFP) into the cationic and Ni-NTA (Ni-nitrilotriacetic acid complex) modified interior [25–28]. Modification of the C-terminal, expected to be directed to the exterior of capsids, enabled the surface modification of artificial viral capsids with gold nanoparticles, coiled-coil peptides, single-stranded DNAs, and proteins [29–34]. Recently, we demonstrated that β-annulus peptide possessing ssDNA at the N-terminal self-assembled into ssDNA-encapsulated artificial viral capsids [35]. Thus, we designed a β-annulus peptide with dT_{20} at the N-terminal to direct mRNA to the interior of capsids via hybridization with poly(A) tails (Figure 1).
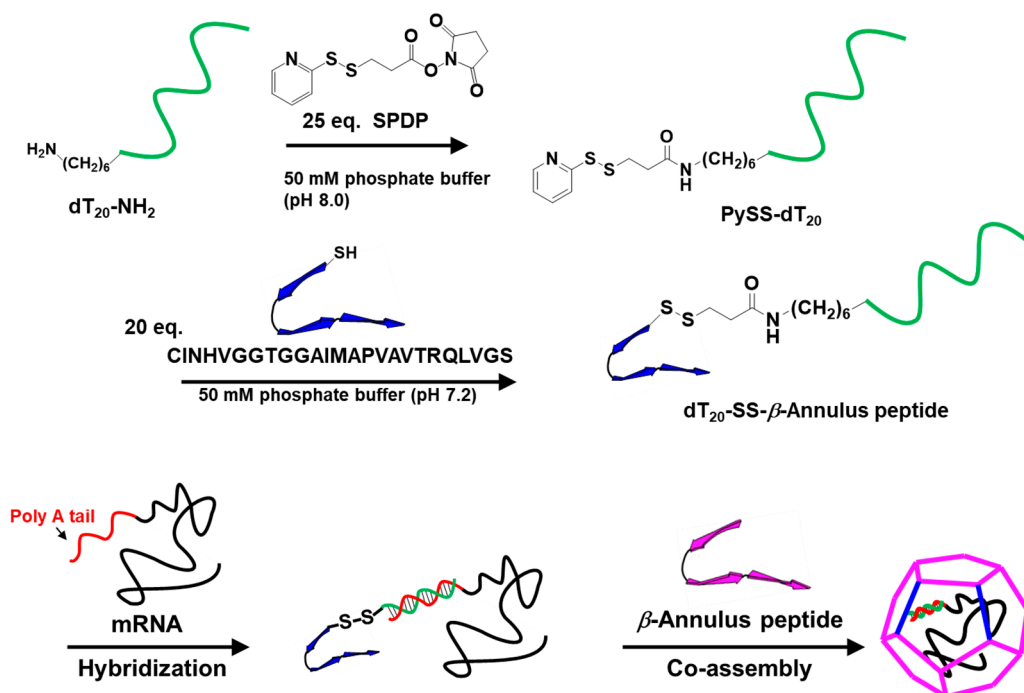
Figure 1. Schematic of synthesis of dT_{20} modified β-annulus peptide (dT_{20}-SS-β-annulus) and formation of an artificial viral capsid by co-assembly of β-annulus peptide and dT_{20}-SS-β-annulus hybridized with mRNA.

2. Materials and Methods

2.1. General

Reverse-phase HPLC was performed at ambient temperature with a Shimadzu LC-6AD liquid chromatograph equipped with a UV–Vis detector (220 nm and 260 nm, Shimadzu SPD-10AVvp, Kyoto, Japan) using an Inertsil WP300 C18 column (GL Science, 250 mm × 4.6 mm or 250 × 20 mm). MALDI-TOF mass spectra were obtained on an Autoflex T2 (Bruker Daltonics, Billerica, USA) in linear/positive mode with α-cyano-4-hydroxycinnamic acid (α-CHCA) or 3-hydroxypicolinic acid (3-HPA) with diammonium hydrogen citrate as the matrix. The UV–Vis spectra of DNA-conjugated peptides were measured at 260 nm using a Jasco V-630 (JASCO Corporation, Tokyo, Japan) with a quartz cell (S10-UV-1, GL Science). An mRNA coding mCherry fluorescent protein (mCherry mRNA, ~1 kb) with a 3'-polyadenylic acid (poly(A)) tail was purchased from OZ Biosciences (Marseille, France). RNase A was purchased from Nacalai Tesque (Kyoto, Japan). All other reagents were obtained from a commercial source and used without further purification. Deionized water of high resistivity (>18 MΩ cm) was purified using a Millipore Purification System (Milli-Q water, Merck Millipore, Burlington, USA) and used as a solvent.

2.2. Preparation of dT$_{20}$-SS-β-Annulus and β-Annulus Peptides

β-annulus (INHVGGTGGAIMAPVAVTRQLVGS) and Cys-β-annulus (CINHVGGTGGAIMA PVAVTRQLVGS) peptides were synthesized with a Biotage Initiator$^+$ (Biotage, Uppsala, Kingdom of Sweden) using standard Fmoc-based coupling chemistry as previously described [22,28]. MALDI-TOF-MS of the β-annulus peptide (matrix: α-CHCA): *m/z* = 2306 (exact mass: 2306) and of the Cys-β-annulus peptide (matrix: α-CHCA): *m/z* = 2409 (exact mass: 2409).

An amine-modified dT$_{20}$ (5′NH$_2$-(CH$_2$)$_6$-TTTTTTTTTTTTTTTTTTTT-3′, Gene Design Inc., Osaka, Japan) in 50 mM sodium phosphate buffer (pH 8.0) was added to 20-fold molar excess of *N*-succinimidyl 3-(2-pyridyldithio)propionate (SPDP) in acetonitrile and the mixture was incubated for 1 h at 25 °C. A Spectra/por7 membrane with a cutoff Mw 1000 (Spectrum Laboratories, Inc., Rancho Dominguez, USA) was used for dialysis against water for 24 h. The internal solution was lyophilized to afford a flocculent solid. This product was dissolved in water and the concentration was defined by UV–Vis spectroscopy. Product (PySS-dT$_{20}$) yield was 43.6 nmol (94.8%)—MALDI-TOF-MS (matrix: 3-HPA): *m/z* = 6409 (exact mass: 6398).

An aqueous solution of PySS-dT$_{20}$ (0.1 mM) in a 50 mM sodium phosphate buffer (pH 7.2) was mixed with the Cys-β-annulus peptide (2 mM) in a 50 mM sodium phosphate buffer (pH 7.2) and the mixture was incubated for 24 h at 25 °C. The solution was purified by reverse-phase HPLC eluted with a linear gradient of CH$_3$CN/0.1 M ammonium formate aqueous solution (10/90 to 100/0 over 95 min). The elution fraction was collected, concentrated in a centrifugal evaporator, and dialyzed as above against water for 20 h. The internal solution was lyophilized to afford a flocculent solid. This product was dissolved in water and the concentration was defined by UV–Vis spectroscopy. Product (dT$_{20}$-SS-β-annulus peptide) yield was 12.6 nmol (27.4%)—MALDI-TOF-MS (matrix: 3-HPA): *m/z* = 8710 (exact mass: 8698).

2.3. Preparation and Characterization of Artificial Viral Capsids

Lyophilized dT$_{20}$-SS-β-annulus and β-annulus peptides were dissolved in water, respectively. Peptide solutions were mixed at molar ratios of dT$_{20}$-SS-β-annulus:β-annulus = 1:9, 1:4.5, 1:2, and 1:1, sonicated for 5 min, and lyophilized. Stock solutions of peptides were prepared by dissolving peptide powders in 1× phosphate buffered saline (PBS, pH 7.4) and sonicating for 3 min.

Dynamic light scattering (DLS) was measured with a Zetasizer NanoZS (Malvern, Kobe, Japan) instrument at 25 °C using an incident He-Ne laser (633 nm). Correlation times of scattered light intensities G(τ) were measured several times and the means were fitted to Equation (1), where *B* is the baseline, *A* is amplitude, *q* is the scattering vector, τ is the delay time, and *D* is the diffusion coefficient.

$$G(\tau) = B + A \exp(-2q^2 D\tau) \tag{1}$$

Hydrodynamic radii (R_H) of scattering particles were calculated using the Stokes-Einstein Equation (2), where η is the solvent viscosity, k_B is Boltzmann's constant, and *T* denotes absolute temperature.

$$R_H = k_B T / 6\pi\eta D \tag{2}$$

Transmission electron microscopy (TEM) images were obtained with a JEOL JEM 1400 Plus (JEOL Ltd., Tokyo, Japan), using an accelerating voltage of 80 kV. Aliquots (5 μL) of DLS samples were applied to hydrophilized carbon-coated Cu-grids (C-SMART Hydrophilic TEM girds, Alliance Biosystems, Osaka, Japan) for 60 s and then removed. Subsequently, the TEM grid was instilled in the aqueous solution (5 μL) of 2% phosphotungstic acid, Na$_3$(PW$_{12}$O$_{40}$)(H$_2$O)$_n$. The staining solution was removed after 60 s and the sample-loaded grids were dried *in vacuo*.

2.4. Preparation of Complex of dT$_{20}$-SS-β-Annulus:β-Annulus Peptide Hybridized with mCherry mRNA

An aqueous solution of mCherry mRNA in 1× PBS (1 mg/mL, (nucleotide) ≈ 3 mM, and pH 7.4) was mixed with dT$_{20}$-SS-β-annulus:β-annulus peptide powders by gentle pipetting without sonication. The peptide solutions were diluted in 1× PBS (pH 7.4) so that the nucleotide concentration of mCherry mRNA was equal to dT$_{20}$ ((mRNA nt) = (T) = 1 mM, (dT$_{20}$) = 50 μM, (RNA) = 1 μM). In a typical experiment, the dT$_{20}$-SS-β-annulus:β-annulus/mRNA solution was incubated for 30 min at 25 °C.

2.5. Electrophoretic Mobility Shift Assay and Nuclease Resistance Assay

Electrophoretic mobility shift assay (EMSA) was employed for the detection of peptide complexes with nucleic acids. The dT$_{20}$-SS-β-annulus:β-annulus/mRNA solutions were loaded onto 3% *w/v* agarose gels in a TAE buffer, pre-cast with GelRed (Wako Pure Chemical Industries, Osaka, Japan) for nucleic acid detection. Three microliters of the dT$_{20}$-SS-β-annulus:β-annulus/mRNA solution ((mRNA nt) = (T) = 1 mM) was loaded with 5 μL of Bluejuice Gel loading buffer (Thermo Ficher, Waltham, USA). Electrophoresis used 210 V for 30 min on an Atto AE-6100 with Atto mypower II300 AE-8130 (Atto, Tokyo, Japan). The bands were visualized with a UV illuminator (TP-15 MP, Atto, Tokyo, Japan) and the images were recorded with a digital camera.

Ribonuclease A from bovine pancreas (Nacalai Tesque, Kyoto, Japan) is an endoribonuclease which specifically hydrolyzes the 3′end of pyrimidine residues in single-stranded RNA. Each peptide/mRNA solution was incubated with a solution of RNase A (3 μL, 1 U/μL) in PBS for 10–60 min at 37 °C. Enzymatic degradation of mRNA was evaluated by EMSA.

2.6. Confocal Laser Scanning Microscopy (CLSM) Measurements of In-Cell Expression of mCherry mRNA

Confocal laser scanning microscopy (CLSM) used a Fluo View FV10i (Olympus, Tokyo, Japan). Human hepatoma HepG2 cells were cultured in DMEM (10 v/v% FBS, 100 μg/mL streptomycin, 100 units/mL penicillin, 1 mM sodium pyruvate, and 1 v/v% MEM nonessential amino acids) for 24 h at 37 °C in a 5% CO$_2$ atmosphere. The cells were seeded onto single-well bottom dishes with 2.0×10^4 cells/well in a final volume of 100 μL and incubated for 24 h at 37 °C and 5% CO$_2$. The medium was removed and 50 μM dT$_{20}$-SS-β-annulus, 450 μM β-annulus, and 1 μM mCherry mRNA in the fresh medium were added to the cells, then incubated for 48 h under 5% CO$_2$. The co-assembly mixture of 50 μM dT$_{20}$-SS-β-annulus, 450 μM β-annulus-His$_{16}$, and 1 μM mCherry mRNA was added to the cells for evaluation of expression of mCherry fluorescent protein. A complex of 2 μM TransIT-mRNA (Transfection kit, Mirus Bio LLC, Madison, USA) with 1 μM mCherry mRNA was added to cells as a positive control. CLSM images of mCherry fluorescence were obtained with excitation at 587 nm and an mCherry band-pass filter (Red). Fluorescence intensity was measured by cell from CLSM images by subtracting background intensity using ImageJ 1.51 software.

3. Results and Discussion

3.1. Synthesis and Self-Assembling Behavior of β-Annulus Peptide Bearing dT$_{20}$ at the N-Terminus

We designed a β-annulus peptide bearing dT$_{20}$ at the N-terminus that was directed to the interior of the capsid (Figure 1) to encapsulate mRNA via hybridization between dT$_{20}$ and the poly(A) tail at the 3′end of mRNA. A 5′-terminal aminated 20-mer thymidine nucleotide (dT$_{20}$-NH$_2$) was reacted with *N*-succinimidyl 3-(2-pyridyldithio)propionate (SPDP) to obtain a dT$_{20}$ bearing pyridyl disulfide group at the 5′-end (PySS-dT$_{20}$). A Cys-β-annulus peptide (CINHVGGTGGAIMAPVAVTRQLVGS) containing Cys at the N-terminus was synthesized by standard Fmoc-based solid-phase methods according to our reported procedure [28]. PySS-dT$_{20}$ was attached to the Cys-β-annulus peptide with a disulfide-exchange reaction. A reversed-phase HPLC chart of the reaction mixture showed one peak at 26.7 min, which was different from the retention time of dT$_{20}$-NH$_2$ and PySS-dT$_{20}$ (Figure 2A). The purified product was assigned by MALDI-TOF-MS as dT$_{20}$-modified β-annulus peptide (dT$_{20}$-SS-β-Annulus) (Figure 2B). DLS of a 50 μM solution of dT$_{20}$-SS-β-annulus in PBS (pH 7.4) exhibited

formation of 77 ± 21 and 40 ± 8 nm assemblies (Figure 2C). TEM images of the aqueous solution stained with phosphotungstic acid showed the formation of spherical assemblies of approximately 40 nm in diameter (Figure 2D). The concentration dependence of the size distribution in DLS measurement indicated that dT_{20}-SS-β-annulus formed assemblies with sizes ranging from 30 to 100 nm in a concentration range of 5–125 μM (Figure S1). This tendency was similar to the findings in our previous report [35]. Notably, β-annulus peptide modified with highly charged dT_{20} formed relatively stable artificial viral capsids.
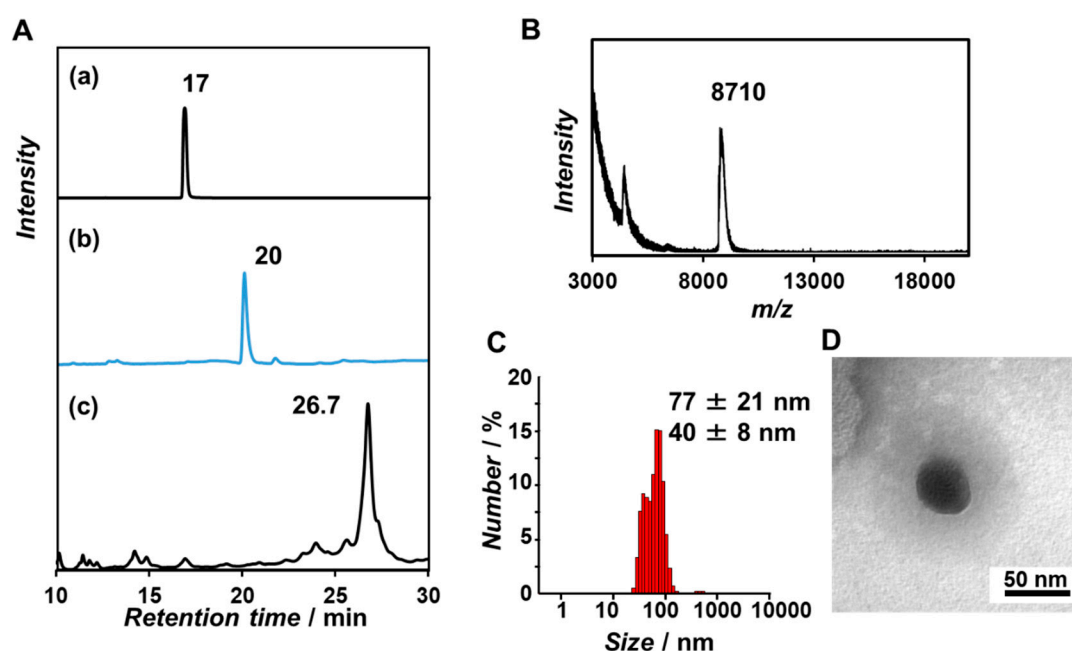
Figure 2. (**A**) Reverse-phase HPLC chart of (**a**) dT_{20}-NH_2, (**b**) PySS-dT_{20} detected at 260 nm, eluted with a linear gradient of CH_3CN/0.1 M NH_4HCO_2 aq (0/100 to 100/0 over 95 min), and (**c**) dT_{20}-SS-β-annulus detected at 260 nm, eluted with a linear gradient of CH_3CN/0.1 M NH_4HCO_2 aq (10/90 to 100/0 over 95 min). (**B**) MALDI-TOF-MS of the purified dT_{20}-SS-β-annulus (matrix: 3-HPA). (**C,D**) TEM image and size distribution obtained from dynamic light scattering (DLS) for an aqueous solution of 50 μM dT_{20}-SS-β-annulus in PBS (pH 7.4) at 25 °C.

3.2. Complexation of mCherry mRNA and Artificial Viral Capsid Bearing dT_{20}

We initially attempted encapsulation of mRNA within the artificial viral capsid consisting of dT_{20}-SS-β-annulus via hybridization between dT_{20} and mRNA. However, when poly(A) and dT_{20}-SS-β-annulus were mixed at equimolar base concentrations, capsid formation was insufficient (data are not shown). It is probably difficult to self-assemble among dT_{20}-SS-β-annulus peptides hybridized on a large poly(A) molecule due to the excluded volume effect. Therefore, we developed an alternate strategy to encapsulate mRNA with dT_{20}-SS-β-annulus and unmodified β-annulus peptide (INHVGGTGGAIMAPVAVTRQLVGS) (Figure 1). DLS and TEM images of the mixture of dT_{20}-SS-β-annulus/unmodified β-annulus peptide at 1:9 molar ratio in PBS showed the formation of spherical co-assemblies of size 45 ± 20 nm (Figure 3). The peptides mixture at other molar ratios (dT_{20}-SS-β-annulus:β-annulus = 1:4.5, 1:2, 1:1) also formed spherical co-assemblies of similar size (Figure S2). Next, we encapsulated mRNA coding in the mCherry fluorescent protein (mCherry mRNA) by co-assembly at different molar ratios of dT_{20}-modified and unmodified β-annulus peptide.
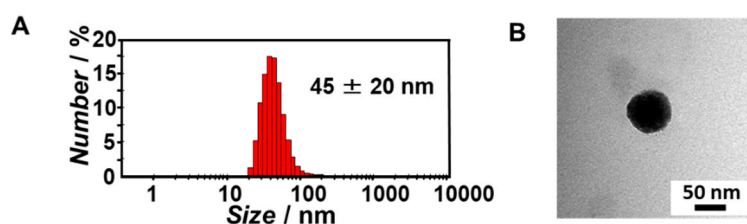
Figure 3. (**A**) Size-distributions obtained from DLS and (**B**) TEM images for co-assembly peptides (dT$_{20}$-SS-β-annulus:β-annulus = 1:9) in water at 25 °C.

An aqueous solution of mCherry mRNA in PBS was added to the lyophilized powder of dT$_{20}$-SS-β-annulus:β-annulus peptide followed by dilution with PBS and incubation for 30 min at 25 °C to prepare capsids containing mCherry mRNA. The electrophoretic mobility shift assay (EMSA) showed a band of mCherry mRNA significantly shifted by complexation with a co-assembly mixture of dT$_{20}$-SS-β-annulus:β-annulus peptide at a 1:9 molar ratio (Figure 4A, lane 4). In contrast, the other co-assembly mixtures showed only a slight retardation of mRNA (Figure 4A, lane 5–7), which reflect almost neutral net charge and relatively small size of the β-annulus peptide. The migration position of a mixed solution of unmodified β-annulus peptide and mCherry mRNA was not shifted from mCherry mRNA alone (Figure 4B). DLS and TEM images of the 1:9 co-assembly complexes with mCherry mRNA show the formation of spherical assemblies of size 52 ± 10 nm (Figure 5A,B). We previously reported that the N-terminus of the β-annulus peptide is directed toward the interior of the capsid and the surface ζ-potential of the capsid is almost zero at neutral pH [25]. Thus, when negatively charged RNA is encapsulated at neutral pH, the artificial viral capsid should minimally migrate from the applied position due to the capsid charge shield. Therefore, EMSA results indicate that the dT$_{20}$-SS-β-annulus:β-annulus peptide 1:9 co-assembly encapsulated mCherry mRNA via hybridization with dT$_{20}$ directed to the interior of capsids. EMSA shows that mCherry mRNA could be complexed with the 1:9 co-assembly at 4 °C, 25 °C, 37 °C, and 60 °C (Figure S3). However, complexation at 4 °C and 60 °C afforded large aggregates with bimodal size distribution (Figure S4). Thus, mCherry mRNA-encapsulated artificial viral capsid with unimodal size distribution can be obtained by incubation with the 1:9 co-assembly mixture at temperatures of 25 °C–37 °C.
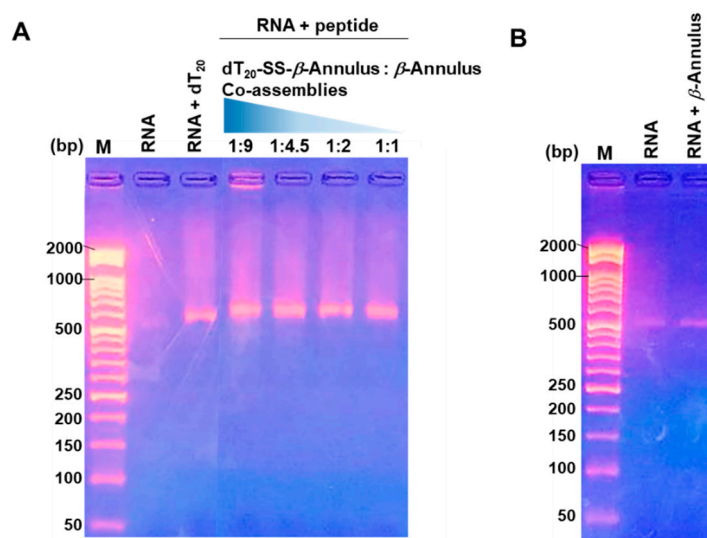
Figure 4. Gel shift assay of (**A**) co-assembly peptides hybridized with mCherry mRNA, (**B**) mixture of β-annulus peptide and mCherry mRNA in phosphate buffered saline (PBS) (pH 7.4) incubated at 25 °C for 30 min. M: DNA marker. All DNA markers used in the gel shift assay are the same. The gels were stained with GelRed.
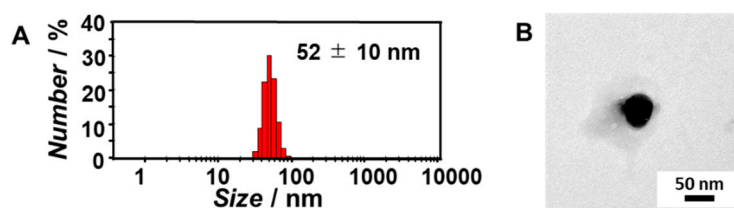
Figure 5. (**A**) Size-distributions obtained from DLS and (**B**) TEM images for co-assembly peptides (dT$_{20}$-SS-β-annulus:β-annulus = 1:9) and mCherry mRNA in PBS (pH 7.4) obtained after incubation at 25 °C.

3.3. Nuclease Resistance of mRNA-Encapsulated Artificial Viral Capsid

Resistance of mCherry mRNA-encapsulated artificial viral capsid to endoribonuclease (RNase A) was confirmed by EMSA. Naked mCherry mRNA was digested by RNase A within 10 min (Figure 6(Aa),B lane 3). Conversely, mRNA in artificial viral capsids (band near the loading well) was minimally digested after 60 min (Figure 6(Ac),B lane 5–8) due to protection by the capsid. For the artificial viral capsids modified with dT$_{20}$, the exteriors were constructed as a control by self-assembly of β-annulus peptide modified with dT$_{20}$ at the C-terminal that directed dT$_{20}$ to the exterior of the capsid. The mixture of mCherry mRNA and the dT$_{20}$-modified capsid at the exterior did not cause a significant mobility shift (Figure 6B lane 9), indicating that mRNA was not encapsulated. mRNA was rapidly digested by RNase A within 10 min (Figure 6(Ac),B lane 10). Thus, mRNA is protected from degradation by artificial viral capsids.
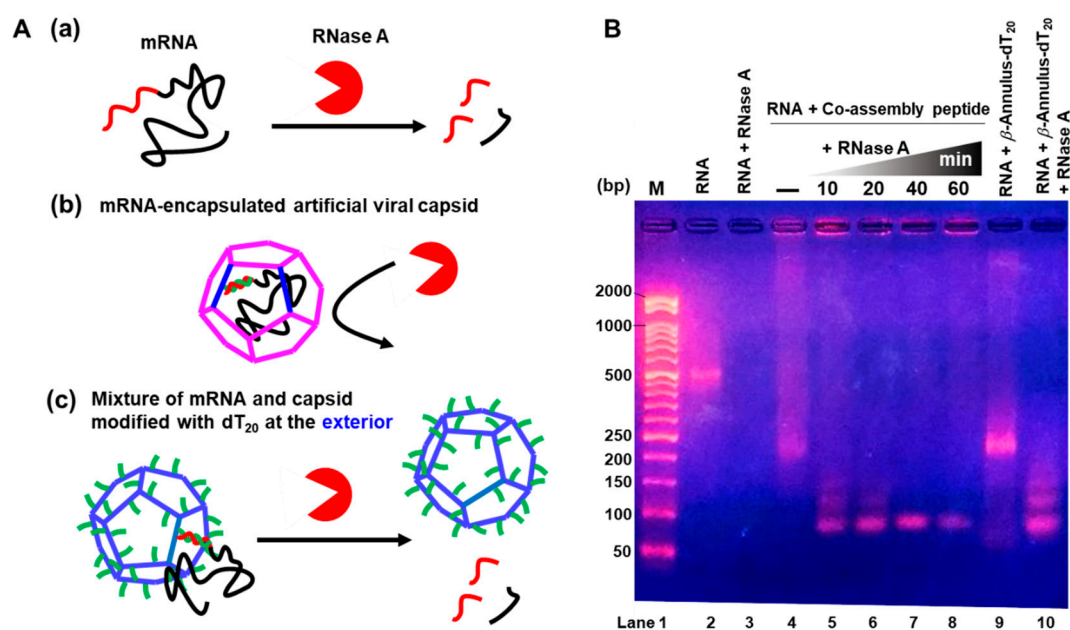
Figure 6. (**A**) Illustration of digestion of mRNA by RNase A: (**a**) mRNA alone, (**b**) mRNA-encapsulated artificial viral capsid, and (**c**) Mixture of mRNA and capsid modified with dT20 at the exterior. (**B**) Gel electrophoresis assay of digestions mRNA by RNase A at 37 °C for 10 min (mRNA alone and β-annulus-dT$_{20}$) and 10–60 min (dT$_{20}$-SS-β-annulus:β-annulus = 1:9 co-assembly). The gel was stained with GelRed.

3.4. In-Cell Expression of mCherry mRNA Encapsulated in Artificial Viral Capsid

Uptake of mCherry mRNA-encapsulated capsids into human hepatoma HepG2 cells were analyzed by CLSM to evaluate mCherry mRNA expression inside cells. mCherry mRNA and a strong transfection reagent (TransIT-mRNA) were incubated with the cells for 48 h at 37 °C as a positive control; significant red fluorescence of mCherry was observed (Figure 7(Aa)). Unfortunately,

minimal expression of encapsulated mCherry mRNA was observed as similar to the naked mCherry mRNA(Figure 7A(b,c)). We employed a histidine 16-mer (His16), a cell-penetrating peptide uncharged under physiological conditions [36,37] to enhance cell permeability of capsids. We constructed artificial viral capsids modified with His16 on the exterior and using the 1:9 co-assembly of dT_{20}-SS-β-annulus peptide and β-annulus peptide modified with His16 at the C-terminal (β-annulus-His16). Significant red fluorescence of mCherry was observed in cells incubated with His16-modified capsids (Figure 7(Ad)). The expression level of mCherry was quantified by fluorescence intensity in the cell areas of the CLSM image using the software ImageJ. The expression level using His16-modified capsids was 26.5 times the expression observed with unmodified capsids (Figure 7B). This indicates that the intracellular expression of mCherry was significantly enhanced by the modification of His16 on the surface of the artificial viral capsid. We have demonstrated in our previous work that the reductive cleavage of the disulfide bond of the artificial viral capsid by dithiothreitol (DTT) caused the controlled-release of ssDNA with the destruction of the capsid [35]. mCherry mRNA was likely released from capsids in the reducing environment in cells.
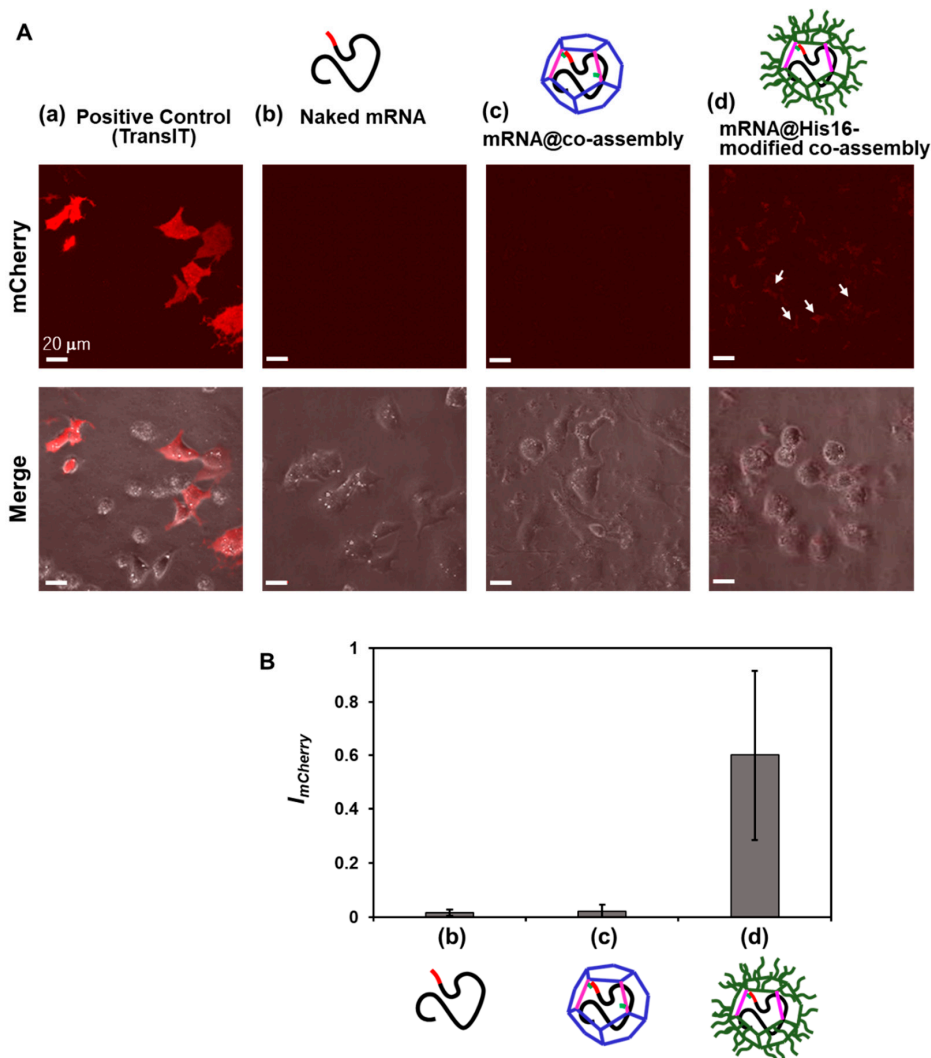
Figure 7. (**A**) Confocal laser scanning microscopy (CLSM) images of HepG2 Cells transfected with mCherry mRNA encapsulated in artificial viral capsids: (**a**) positive control (2 μM TransIT-mRNA with 1 μM mCherry mRNA), (**b**) 1 μM Naked mCherry mRNA, (**c**) mRNA-encapsulated artificial viral capsid (50 μM dT_{20}-SS-β-annulus, 450 μM β-annulus, and 1 μM mCherry mRNA), and (**d**) mRNA-encapsulated histidine 16-mer (His16)-artificial viral capsid (50 μM dT_{20}-SS-β-annulus, 450 μM β-annulus-His16, and 1 μM mCherry mRNA). (**B**) Relative fluorescence intensity of mCherry from HepG2 Cells.

4. Conclusions

We constructed artificial viral capsids co-assembled from viral *β*-annulus peptides bearing dT_{20} at the N-terminus and unmodified peptides. Capsids bearing interior dT_{20} enable encapsulation of mCherry mRNA bearing poly(A) tails via hybridization to form ribonuclease resistant spherical assemblies of approximately 50 nm in diameter. Further, we demonstrate novel material for mRNA delivery by His16-modification on the exterior of capsids. Further research will demonstrate potential applications for artificial viral capsids as delivery systems for nucleic acid drugs.

Supplementary Materials: The following are available online at http://www.mdpi.com/2076-3417/10/22/8004/s1, Figure S1: Concentration dependence of size distribution obtained from DLS for the aqueous solution of dT_{20}-SS-*β*-annulus in PBS (pH7.4) at 25 °C, Figure S2: Size-distributions obtained from DLS and TEM images for co-assembly peptides (dT_{20}-SS-*β*-annulus:*β*-annulus = 1:4.5 (a), 1:2 (b), and 1:1 (c) in water at 25 °C), Figure S3: Gel shift assay obtained after hybridization of co-assembly peptides and mCherry mRNA in PBS (pH 7.4) incubated at various temperatures for 10–30 min, and Figure S4: Size-distributions obtained from DLS and TEM images for co-assembly peptides (dT_{20}-SS-*β*-annulus:*β*-annulus = 1:9) and mCherry mRNA in PBS buffer (pH 7.4) obtained after incubation at 4 °C (a), 37 °C (b), and 60 °C (c) for 10–30 min.

Author Contributions: Conceptualization, K.M.; methodology, T.I. and H.I.; investigation, Y.N. and Y.S.; writing, Y.N. and K.M.; visualization, Y.S. and H.I.; supervision, K.M.; funding acquisition, K.M. All authors have read and agreed to the published version of the manuscript.

Funding: This research was funded by a Grant-in-Aid for Scientific Research on Innovative Areas "Chemistry for Multimolecular Crowding Biosystems" (grant number: JP18H04558) and a Grant-in-Aid for Scientific Research (B) (grant number: JP18H02089).

Conflicts of Interest: The authors declare no conflict of interest.

References

1. Sahin, U.; Karikó, K.; Türeci, Ö. mRNA-based therapeutics—Developing a new class of drugs. *Nat. Rev. Drug Discov.* **2014**, *13*, 759–780. [CrossRef] [PubMed]
2. Yin, H.; Kanasty, R.L.; Eltoukhy, A.A.; Vegas, A.J.; Dorkin, J.R.; Anderson, D.G. Non-viral vectors for gene-based therapy. *Nat. Rev. Genet.* **2014**, *15*, 541–555. [CrossRef] [PubMed]
3. Kauffman, K.J.; Webber, M.J.; Anderson, D.G. Materials for non-viral intracellular delivery of messenger RNA therapeutics. *J. Control. Release* **2016**, *240*, 227–234. [CrossRef] [PubMed]
4. Guan, S.; Rosenecker, J. Nanotechnologies in delivery of mRNA therapeutics using non-viral vector-based delivery systems. *Gene Ther.* **2017**, *24*, 133–143. [CrossRef] [PubMed]
5. Kowalski, P.S.; Rudra, A.; Miao, L.; Anderson, D.G. Delivering the Messenger: Advances in Technologies for Therapeutic mRNA Delivery. *Mol. Ther.* **2019**, *27*, 710–728. [CrossRef]
6. Meng, C.; Chen, Z.; Li, G.; Welte, T.; Shen, H. Nanoplatforms for mRNA Therapeutics. *Adv. Ther.* **2020**. [CrossRef]
7. Uchida, H.; Itaka, K.; Nomoto, T.; Ishii, T.; Suma, T.; Ikegami, M.; Miyata, K.; Oba, M.; Nishiyama, N.; Kataoka, K. Modulated Protonation of Side Chain Aminoethylene Repeats in N-Substituted Polyaspartamides Promotes mRNA Transfection. *J. Am. Chem. Soc.* **2014**, *136*, 12396–12405. [CrossRef]
8. Baba, M.; Itaka, K.; Kondo, K.; Yamasoba, T.; Kataoka, K. Treatment of neurological disorders by introducing mRNA In Vivo using polyplex nanomicelles. *J. Control. Release* **2015**, *201*, 41–48. [CrossRef]
9. Matsui, A.; Uchida, S.; Ishii, T.; Itaka, K.; Kataoka, K. Messenger RNA-based therapeutics for the treatment of apoptosis-associated diseases. *Sci. Rep.* **2015**, *5*, 15810. [CrossRef]
10. Li, J.; Wang, W.; He, Y.; Li, Y.; Yan, E.Z.; Zhang, K.; Irvine, D.J.; Hammond, P.T. Structurally Programmed Assembly of Translation Initiation Nanoplex for Superior mRNA Delivery. *ACS Nano* **2017**, *11*, 2531–2544. [CrossRef]
11. Benner, N.L.; McClellan, R.L.; Turlington, C.R.; Haabeth, O.A.W.; Waymouth, R.M.; Wender, P.A. Oligo(serine ester) Charge-Altering Releasable Transporters: Organocatalytic Ring-Opening Polymerization and their Use for In Vitro and In Vivo mRNA Delivery. *J. Am. Chem. Soc.* **2019**, *141*, 8416–8421. [CrossRef] [PubMed]
12. Rein, A. Retroviral RNA packaging: A review. In *Positive-Strand RNA Viruses*; Brinton, M.A., Calisher, C.H., Rueckert, R., Eds.; Springer: Vienna, Austria, 1994; Volume 9, pp. 513–522.
13. Perlmutter, J.D.; Hagan, M.F. Mechanisms of Virus Assembly. *Annu. Rev. Phys. Chem.* **2015**, *66*, 217–239. [CrossRef] [PubMed]
14. Azuma, Y.; Edwardson, T.G.W.; Terasaka, N.; Hilvert, D. Modular Protein Cages for Size-Selective RNA Packaging in Vivo. *J. Am. Chem. Soc.* **2018**, *140*, 566–569. [CrossRef] [PubMed]

15. Terasaka, N.; Azuma, Y.; Hilvert, D. Laboratory evolution of virus-like nucleocapsids from non-viral protein cages. *Proc. Natl. Acad. Sci. USA* **2018**, *115*, 5432–5437. [CrossRef]

16. Munroe, D.; Jacobson, A. Tales of poly(A): A review. *Gene* **1990**, *91*, 151–158. [CrossRef]

17. Sachs, A. The role of poly(A) in the translation and stability of mRNA. *Curr. Opin. Cell Biol.* **1990**, *2*, 1092–1098. [CrossRef]

18. Eckmann, C.R.; Rammelt, C.; Wahle, E. Control of poly(A) tail length. *Wiley Interdiscip. Rev. RNA* **2011**, *2*, 348–361. [CrossRef]

19. Weill, L.; Belloc, E.; Bava, F.-A.; Méndez, R. Translational control by changes in poly(A) tail length: Recycling mRNAs. *Nat. Struct. Mol. Biol.* **2012**, *19*, 577–585. [CrossRef]

20. Gruber, A.J.; Zavolan, M. Alternative cleavage and polyadenylation in health and disease. *Nat. Rev. Genet.* **2019**, *20*, 599–614. [CrossRef]

21. Nicholson, A.L.; Pasquinelli, A.E. Tales of Detailed Poly(A) Tails. *Trends Cell Biol.* **2019**, *29*, 191–200. [CrossRef]

22. Matsuura, K.; Watanabe, K.; Matsuzaki, T.; Sakurai, K.; Kimizuka, N. Self-Assembled Synthetic Viral Capsids from a 24-mer Viral Peptide Fragment. *Angew. Chem. Int. Ed.* **2010**, *49*, 9662–9665. [CrossRef]

23. Matsuurua, K. Rational design of self-assembled proteins and peptides for nano and micro-sized architectures. *RSC Adv.* **2014**, *4*, 2942–2953. [CrossRef]

24. Matsuura, K. Synthetic approaches to construct viral capsid-like spherical nanomaterials. *Chem. Commun.* **2018**, *54*, 8944–8959. [CrossRef]

25. Matsuura, K.; Watanabe, K.; Matsushita, Y.; Kimizuka, N. Guest-binding behavior of peptide nanocapsules self-assembled from viral peptide fragments. *Polym. J.* **2013**, *45*, 529–534. [CrossRef]

26. Fujita, S.; Matsuura, K. Inclusion of zinc oxide nanoparticles into virus-like peptide nanocapsules self-assembled from viral β-annulus peptide. *Nanomaterials* **2014**, *4*, 778–791. [CrossRef]

27. Fujita, S.; Matsuura, K. Encapsulation of CdTe Quantum Dots into Synthetic Viral Capsids. *Chem. Lett.* **2016**, *45*, 922–924. [CrossRef]

28. Matsuura, K.; Nakamura, T.; Watanabe, K.; Noguchi, T.; Minamihata, K.; Kamiya, N.; Kimizuka, N. Self-assembly of Ni-NTA-modified β-annulus peptides into artificial viral capsids and encapsulation of His-tagged proteins. *Org. Biomol. Chem.* **2016**, *14*, 7869–7874. [CrossRef]

29. Matsuura, K.; Ueno, G.; Fujita, S. Self-assembled artificial viral capsid decorated with gold nanoparticles. *Polym. J.* **2014**, *47*, 146–151. [CrossRef]

30. Nakamura, Y.; Yamada, S.; Nishikawa, S.; Matsuura, K. DNA-modified artificial viral capsids self-assembled from DNA-conjugated β-annulus peptide. *J. Pept. Sci.* **2017**, *23*, 636–643. [CrossRef]

31. Matsuura, K.; Matsuura, K. Self-assembled artificial viral capsids bearing coiled-coils at the surface. *Org. Biomol. Chem.* **2017**, *15*, 5070–5077. [CrossRef]

32. Matsuura, K.; Honjo, T. Artificial Viral Capsid Dressed Up with Human Serum Albumin. *Bioconjug. Chem.* **2019**, *30*, 1636–1641. [CrossRef] [PubMed]

33. Matsuura, K.; Ota, J.; Fujita, S.; Shiomi, Y.; Inaba, H. Construction of Ribonuclease-Decorated Artificial Virus-like Capsid by Peptide Self-assembly. *J. Org. Chem.* **2019**, *85*, 1668–1673. [CrossRef] [PubMed]

34. Matsuura, K. Dressing up artificial viral capsids self-assembled from C-terminal-modified β-annulus peptides. *Polym. J.* **2020**, *52*, 1035–1041. [CrossRef]

35. Nakamura, Y.; Inaba, H.; Matsuura, K. Construction of Artificial Viral Capsids Encapsulating Short DNAs via Disulfide Bonds and Controlled Release of DNAs by Reduction. *Chem. Lett.* **2019**, *48*, 544–546. [CrossRef]

36. Iwasaki, T.; Tokuda, Y.; Kotake, A.; Okada, H.; Takeda, S.; Kawano, T.; Nakayama, Y. Cellular uptake and In Vivo distribution of polyhistidine peptides. *J. Control. Release* **2015**, *210*, 115–124. [CrossRef] [PubMed]

37. Hayashi, T.; Shinagawa, M.; Kawano, T.; Iwasaki, T. Drug delivery using polyhistidine peptide-modified liposomes that target endogenous lysosome. *Biochem. Biophys. Res. Commun.* **2018**, *501*, 648–653. [CrossRef]